

**FINAL REPORT**

**CROSSFLOW SAMPLER FOULING INDEX**

**MWH**  
**300 N. Lake Avenue, Suite 1200**  
**Pasadena, CA 91101**



**MWH**  
MONTGOMERY WATSON HARZA

**CROSSFLOW SAMPLER FOULING INDEX**

**FINAL REPORT**

Prepared by

**Samer Adham, Ph.D.**  
MWH Americas Inc.,  
300 N. Lake Boulevard, Suite 1200  
Pasadena, CA 91101

and

**Tony Fane, Ph.D.**  
205, Applied Science Building  
University of New South Wales  
Sydney, 2052, Australia

Sponsored by:  
National Water Research Institute

September 2007

## ACKNOWLEDGEMENTS

The project team would like to thank the National Water Research Institute for funding the project. Sincere thanks to Gil Hurwitz (UCLA), Li Liu (MWH), and Arun Subramani (MWH) for providing assistance to the project.

## TABLE OF CONTENTS

List of Figures	5
List of Tables	6
<b>1. INTRODUCTION</b>	7
<b>2. THEORY</b>	8
<b>3. MATERIALS AND METHODS</b>	9
3.1. <i>Feed Water</i>	9
3.2. <i>Cross flow Sampler (CFS) Setup</i>	10
3.3. <i>Silt Density Index (SDI)</i>	11
3.4. <i>Modified Fouling Index (MFI)</i>	11
<b>4. CHALLENGES IN MEASUREMENT TECHNIQUE</b>	13
4.1. <i>Control experiment with deionized water</i>	13
4.2. <i>Control experiment with deionized water and sodium hypochlorite</i>	15
<b>5. RESULTS AND DISCUSSION</b>	17
5.1. <i>Influence of conventional pretreatment</i>	17
5.2. <i>Influence of loose MF/tight conventional pretreatment</i>	20
5.3. <i>Influence of MF pretreatment</i>	20
5.4. <i>Influence of tight UF pretreatment</i>	22
<b>6. CONCLUSIONS</b>	26
<b>7. FUTURE WORK</b>	27

## LIST OF FIGURES

<i>Figure Description</i>	<i>Page Number</i>
<b>Figure 1.</b> Back-transport velocity of particles in microfiltration of colloidal particles as a function of particle diameter (adapted from Wiesner et al, 1988) is shown in (a) and in (b) a similar analysis for conditions in a spiral wound RO module is illustrated.	9
<b>Figure 2.</b> Schematic diagram of the cross-flow sampler (CFS) setup.	11
<b>Figure 3.</b> Ratio of filtration and volume as a function of the total volume of filtrated feed water indicating the three dominant filtration mechanisms: blocking filtration, cake filtration, and cake filtration.	13
<b>Figure 4.</b> SDI (a) and MFI (b) measurements for control experiment with DI water.	14
<b>Figure 5.</b> SDI (a) and MFI (b) measurements for control experiment with DI water and chlorine.	16
<b>Figure 6.</b> Influence of conventional (1 $\mu\text{m}$ ) pretreatment on SDI (a) and MFI (b) measurements for San Diego bay seawater and SPW surface water before and after CFS. Number of experiments conducted for each source water, $n = 2$ .	18
<b>Figure 7.</b> Illustration of cake layer structure in the presence of wide particle size distribution is shown in (a) and in (b) cake layer structure in the presence of uniform particle size distribution is shown.	19
<b>Figure 8.</b> Illustration of hypothesized particle size distribution obtained from CFS filtrate.	20
<b>Figure 9.</b> Influence of loose MF/tight conventional (0.22 $\mu\text{m}$ ) pretreatment on SDI (a) and MFI (b) measurements for San Diego bay seawater and SPW surface water before and after CFS. Number of experiments conducted for each source water, $n = 2$ .	21
<b>Figure 10.</b> Influence of loose MF (0.1 $\mu\text{m}$ ) pretreatment on SDI (a) and MFI (b) measurements for MBR effluent before and after CFS. Number of experiments conducted for each source water, $n = 2$ .	22
<b>Figure 11.</b> Influence of tight UF (0.04 $\mu\text{m}$ ) pretreatment on SDI (a) and MFI (b) measurements for SPW surface water before and after CFS. Number of experiments conducted for each source water, $n = 2$ .	24
<b>Figure 12.</b> Comparison between conventional SDI and SDI-CFS measurements (a) and (b) comparison between conventional MFI and MFI-CFS measurements.	25

**LIST OF TABLES**

*Table Description*

*Page Number*

**Table 1.** Characteristics of Prefiltration Membranes.

10

## 1. INTRODUCTION

Membrane fouling is an important concern in the design and operation of membrane systems for water and wastewater treatment. Particulate fouling of reverse osmosis (RO) and nanofiltration (NF) membranes is of major concern due to a decrease in plant productivity and increased operational costs associated with higher applied pressure requirements and frequent use of chemical cleaning agents. Various fouling indices have been developed in the past to provide an indication of membrane fouling potential. Most commonly used indices for determining the suitability of feedwater for RO treatment are the silt density index (SDI) and the modified fouling index (MFI) (MWH, 2005).

Although various fouling indices have been developed in the past, there are several drawbacks associated with the standard methods. Since the standard SDI and MFI measurements are conducted using a 0.45  $\mu\text{m}$  filter, later studies were conducted in order to capture the effect of the smaller particulates and macromolecules. Thus, the  $\text{MFI}_{\text{UF}}$  index was proposed. The index uses a smaller pore size ultrafiltration membrane with a molecular weight cut off (MWCO) of 13,000 KDa (Boerlage et al., 2000). All of the above mentioned standard indices are based on filtration of water in dead end mode. In contrast, RO processes involve the use of cross flow velocity to reduce the effect of fouling and concentration polarization. Thus, the influence of cross flow hydrodynamics is not considered in previous fouling indices. Both SDI and MFI measurements are conducted using a 0.45  $\mu\text{m}$  filter. In a cross flow RO module, particles with a certain size distribution will have a higher probability of depositing and causing the observed fouling. Additionally, the effect of turbulence promoting spacers that are commonly used in RO applications is not considered when a dead end filtration approach is used. Thus, the standard fouling indices are not representative of cake filtration occurring in actual RO processes. Finally, standard fouling indices are usually conducted under constant pressure. Whereas in contrast, most RO plants operate under constant flux conditions in order to maintain plant productivity.

Due to the various drawbacks associated with the previously developed fouling indices, this project involves the development of a novel method that can be considered as a more representative index of particulate RO fouling. The current method used in this project involves the selective removal of particles, that are most likely to deposit and cause fouling, using a cross flow sampler (CFS) operating under the similar cross flow conditions that represent most RO processes. The primary objective is to study the influence of the CFS system on SDI and MFI for different source water types and compare with standardized indices. With the development of such a technique, the CFS could be potentially employed upstream of the fouling index test cell to further improve the correlation between the SDI index and RO fouling potential.

## 2. THEORY

Particle size is an important parameter influencing the transport of particles to and away from membrane surfaces. Wiesner et al. (1988) emphasized the importance of particle size in cross flow filtration by illustrating the influence of particle size back-transport velocity. The back-transport velocity can be related to the probability of deposition of particles leading to fouling. Due to permeation of water through the membrane, there exists convective flux of particles normal to the membrane surface. The net particle velocity normal to the membrane surface arises from a combination of normal and tangential convection along with the back-transport velocity associated with Brownian diffusion (Wiesner et al., 1988). The effect of tangential convection on the transport of a particle to a membrane surface may be described by two processes, shear-induced diffusion and lateral (inertial) lift, which act normal to and away from the membrane surface. The net particle velocity ( $v_p$ ) is a balance between permeate water velocity ( $v_w$ ), lateral (or inertial lift) velocity ( $v_L$ ), shear-induced diffusion velocity ( $v_s$ ), and Brownian diffusion velocity ( $v_B$ ). Thus, the net particle velocity (flux) from the bulk to the membrane surface can be expressed as follows,

$$v_p = v_w - v_L - v_s - v_B \quad (1)$$

The different velocities in equation (1) can be calculated using the following expressions (Wiesner et al., 1998),

$$v_w = \frac{Q}{A_m} \quad (2)$$

$$v_L = \frac{U_0^2 a_p^3 \rho}{4\mu h^2} \quad (3)$$

$$v_s = \frac{0.05U_0 a_p^2}{2h^2} \quad (4)$$

$$v_B = \frac{kT}{12\pi\mu h a_p} \quad (5)$$

In the above equations  $Q$  is the flow rate,  $A_m$  is the membrane area,  $U_0$  is the average cross flow velocity,  $d_p$  is the particle diameter,  $\mu$  is the absolute viscosity,  $\rho$  is the density,  $h$  is the channel height,  $k$  is the Boltzmann's constant,  $T$  is the absolute temperature. According to equations 3-5, the back-transport mechanisms are influenced by particle size, cross flow velocity, and channel geometry with the predominant mechanism determined largely by particle size. Brownian diffusion decreases with increase in particle size whereas inertial lift and shear induced diffusion increase with increasing particle size. Among the back-transport velocities, Brownian diffusion plays an important role for particle diameters smaller than 0.5 microns, inertial lift is important for particle diameter greater than 20 microns, and shear-induced diffusion is dominant for particle diameter in the intermediate range. The concept of back-transport velocities is illustrated in Figure 1 (a) which is reproduced based on the data presented by Wiesner et

al. (1998). Figure 1(b) represents the results from employing a similar analysis for a RO process.

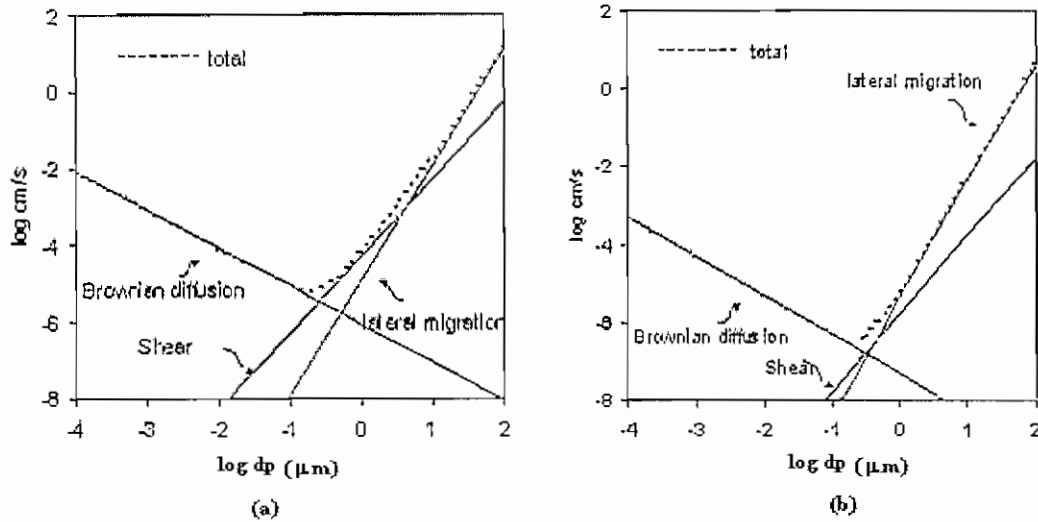


**Figure 1.** Back-transport velocity of particles in microfiltration of colloidal particles as a function of particle diameter (adapted from Wiesner et al, 1988) is shown in (a) and in (b) a similar analysis for conditions in a spiral wound RO module is illustrated.

The above analysis indicates that the lowest velocity and hence the highest probability for deposition occurs around a particle size of 0.2 microns, which is smaller than the 0.45 micron filter employed by the traditional SDI and MFI methods. The analysis showed that the flow characteristics affected the back-transport velocities. Figure 1 (b) shows that the predicted lowest back-transport velocity in a RO system could be an order of magnitude lower than that in MF fibers.

### 3. MATERIALS AND METHODS

#### 3.1. Feed Water

In this study, three different types of water were tested including California state project surface water, San Diego Bay sea water, and a membrane bioreactor (MBR) effluent. The water samples were collected in 20 L containers and transported with blue-ice packs to MWH Research Center and Fabrication Facility in Monrovia, CA. Once received, the samples were stored in 4°C to inhibit biological activity. In order to minimize any changes in the water composition, the experiments were scheduled immediately after receipt of the water.

The raw waters represent three different water sources that are typical influents to a RO process. California State Project Water (SPW), representing surface water source, was provided by the Water Facilities Authority, Agua de Lejos Water Treatment Plant in Upland, California. San Diego Bay Water (SDBW) was natural seawater collected from San Diego Bay, CA. The MBR effluent was collected from the MBR pilot (nominal

membrane pore size of 0.1  $\mu\text{m}$ ) treating municipal wastewater at Point Loma Wastewater Treatment Plant, San Diego, CA.

For all the experiments conducted, surface water and seawater have been prefiltered using different grades of membrane filters. The nominal pore size of these membranes was deliberately selected to represent the different types of pretreatment commonly used for RO processes. The nominal size range of filtration from conventional media filtration is considered to be 1  $\mu\text{m}$ , while 0.22  $\mu\text{m}$  prefiltration is considered as tight conventional media filtration or loose microfiltration. Additionally, the MBR has a nominal membrane pore size of 0.1  $\mu\text{m}$ , which is in the range for most commercially available microfiltration membranes. Finally, filtrate water was collected from an US Filter membrane pilot with a nominal pore size of 0.04  $\mu\text{m}$ , operating on the SPW at Upland, California. The size range for most commercially available ultrafiltration membranes is 0.04  $\mu\text{m}$ . The characteristics of prefiltration membranes are provided in Table 1.

**Table 1.** Characteristics of Prefiltration Membranes

Nominal pore size	Membrane configuration	Pretreatment Type	Source Water
1 $\mu\text{m}$	Cartridge	Conventional media filtration	SPW, SDBW
0.22 $\mu\text{m}$	Flat-sheet	Excellent conventional/ Loose microfiltration	SPW, SDBW
0.1 $\mu\text{m}$	Hollow fiber	Microfiltration	MBR
0.04 $\mu\text{m}$	Hollow fiber	Ultrafiltration	SPW

Note: SPW: California State Project water; SDBW: San Diego Bay sea water; MBR: Membrane Bioreactor effluent.

### 3.2. Cross flow Sampler (CFS) Setup

A schematic diagram of the Cross Flow Sampler (CFS) setup is shown in Figure 2. The major component of this setup was a single-channel cross flow unit accommodating a microsieve. The cross flow channel has dimensions of 2 mm, 146 mm and 95 mm for channel height, length, and width, respectively. Feed spacers (1.65 mm) were placed to promote turbulence and enhance mass transport. The microsieve accommodated in the cross flow unit was a 5  $\mu\text{m}$  GE PCTE (polycarbonate) membrane of 140  $\text{cm}^2$  (22-in.<sup>2</sup>) filtration area. The pore size (5  $\mu\text{m}$ ) is much larger than the prefiltration employed and is not expected to affect results from subsequent experiments. Moreover, the PCTE membrane had straight-through pores. The particles that were deposited on the membrane surface should all pass to the permeate side since no depth-filtration would occur with the straight-through microsieve.

The CFS unit was operated under similar hydrodynamic conditions as a typical RO process to simulate particle deposition. A centrifugal pump (model AC-2CP-MD, March Manufacturing Inc., Glenview, IL) was used to pump the feed solution. For all the experiments, a cross flow rate of 2.0 L/min (equivalent to 1 m/s) was maintained. A peristaltic pump in the permeate line was used to maintain constant flux of 23.4 liters per square meter per hour (LMH), equivalent to 14 gallons per square foot per day (gfd). Remaining feed water was returned to the feed tank. After each experimental run, 2 to 4 liters of CFS permeate was collected to determine SDI and MFI.

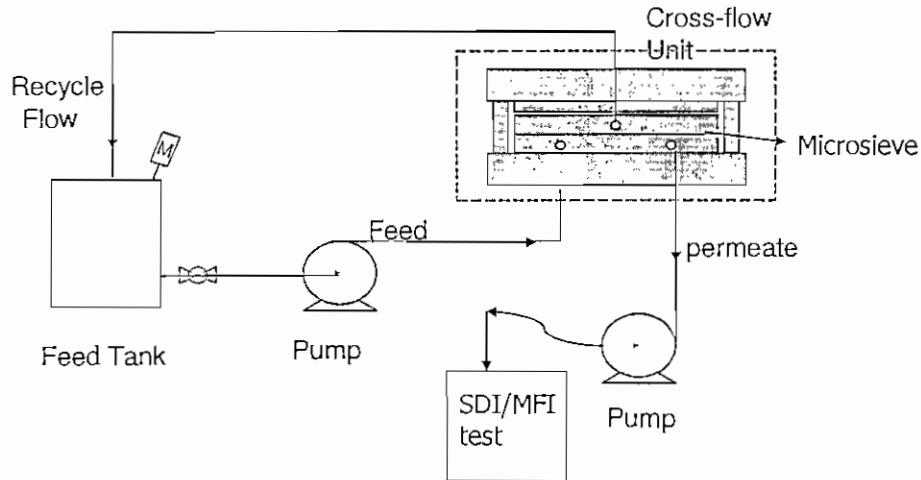


Figure 2. Schematic diagram of the cross flow sampler (CFS) setup.

### 3.3. Silt Density Index (SDI)

The SDI measurements are an indication of the quantity of particulate matter in water (ASTM D4189-95). To measure SDI using the standard method, water is passed through a 0.45  $\mu\text{m}$  membrane filter at a constant applied gage pressure of 207 kPa (30 psi), and the rate of plugging the filter is measured. The SDI is then calculated from the rate of plugging using the following equation,

$$SDI = \frac{100 \left( 1 - \frac{t_i}{t_f} \right)}{t} \quad (6)$$

where  $t_i$  = time to collect initial 500 mL of sample  
 $t_f$  = time to collect final 500 mL of sample  
 $t$  = total running time of test

### 3.4. Modified Fouling Index (MFI)

The MFI is determined using the same equipment and procedure used for the SDI, except that the volume is measured every 30 seconds over a 15 minute filtration period.

MFI was developed based on Darcy's law, which relates the flux to the thickness of the cake layer (Schippers and Verdouw, 1980). The total resistance to flow is the sum of the filter ( $R_m$ ) and cake resistance ( $R_c$ ). Thus, a change in the flux ( $dV/dt$ ) is related to the applied pressure ( $\Delta P$ ) through the total resistance ( $R_m+R_c$ ) as follows,

$$\frac{dV}{dt} = \frac{\Delta P}{\mu} \frac{A_m}{(R_m + R_c)} \quad (7)$$

$$t = \frac{\mu V R_m}{\Delta P A_m} + \frac{\mu V^2 \alpha C_b}{2 \Delta P A_m^2} \quad (8)$$

$$\frac{t}{V} = \frac{\mu R_m}{\Delta P A_m} + \frac{\mu V \alpha C_b}{2 \Delta P A_m^2} \quad (9)$$

$$\frac{1}{Q} = a + MFI \times V \quad (10)$$

where  $V$  is the total permeate produced  
 $\Delta P$  is the transmembrane pressure  
 $\mu$  is the dynamic viscosity of water  
 $A_m$  is the membrane area  
 $R_m$  is the membrane/filter resistance  
 $R_c$  is the cake layer resistance  
 $\alpha$  is the specific cake resistance  
 $C_b$  is the concentration of particles  
 $Q$  is the average flow  
 $a$  is a constant

The above equations predict that a linear relationship exists between  $t/V$  and  $V$  during cake filtration. The slope of the linear region is the MFI. In Figure 3, a typical filtration curve is shown. The first region represents pore blocking (blocking filtration), second region represents cake filtration, and the third region represents cake filtration with compression and/or clogging. The slope of the linear region (cake filtration) represents MFI. To obtain a qualitative comparison of fouling indices before/after the use of CFS, a PALL (25 mm, 0.45  $\mu\text{m}$ ) nylon based filter was used to determine the SDI and MFI. Since the diameter of the filter used was smaller, the permeate collected during the SDI and MFI measurements were scaled down to ~140 mL.

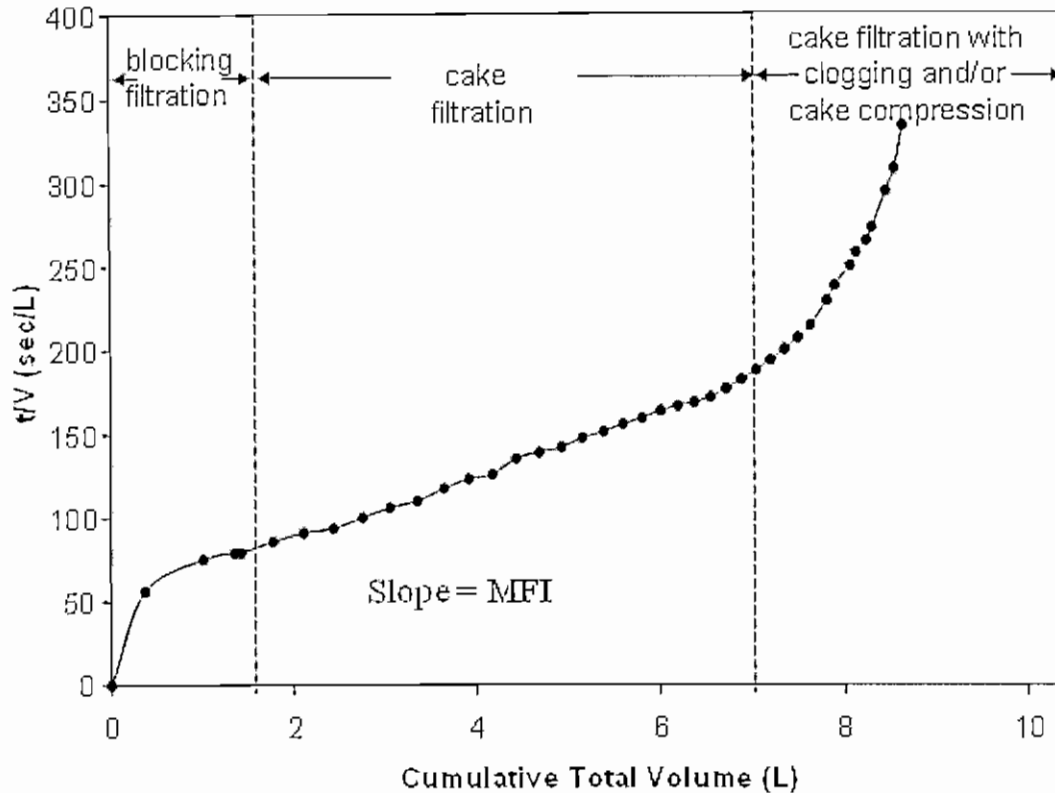


**Figure 3.** Ratio of filtration and volume as a function of the total volume of filtrated feed water indicating the three dominant filtration mechanisms: blocking filtration, cake filtration, and cake filtration with clogging.

#### 4. CHALLENGES IN MEASUREMENT TECHNIQUE

##### 4.1. Control experiment with deionized water

Deionized water (DI) was first used as the feed to CFS to establish the blank control. It was expected that the SDI/MFI of the deionized water before and after CFS would be similar, since apparently no particles were present in deionized water. However, with the current CFS settings, a substantial increase in MFI/SDI values was observed for deionized water after CFS (Figure 4). This indicates potential contamination during the CFS operation.

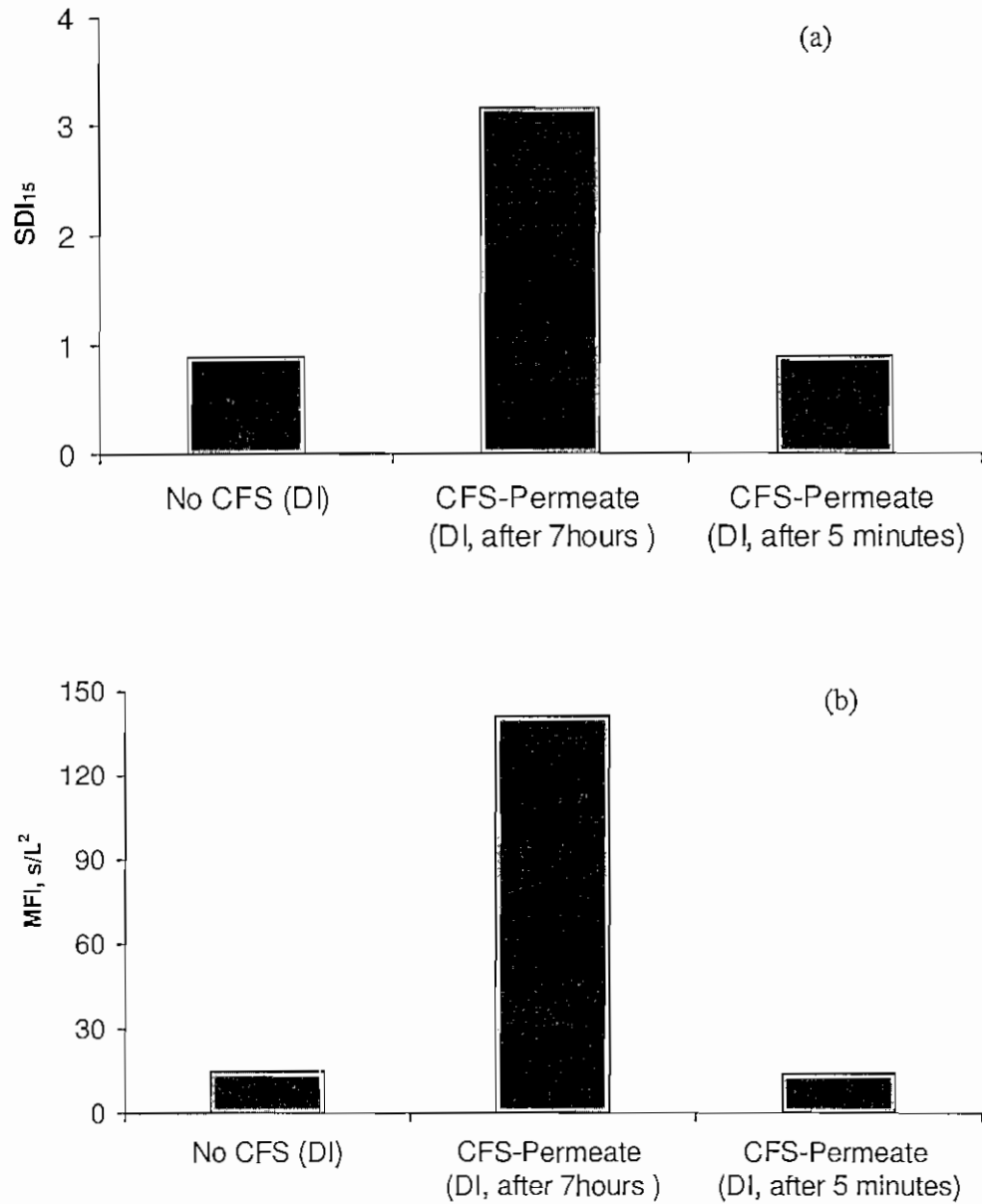


**Figure 4.** SDI (a) and MFI (b) measurements for control experiment with DI water.

The contamination was likely caused by the biological growth during the CFS operation. To simulate the RO operation the CFS permeate flux was kept low at 14 gfd. Since the CFS filter area is  $\sim 0.014 \text{ m}^2$ , to generate enough 2.5 liters of water for the SDI/MFI measurement, seven hours of CFS operation was necessary. During this long cross flow filtration and recirculation period, excess growth of bacteria might occur and eventually cause the increase of SDI/MFI in the CFS permeate. This is confirmed with the third column in Figure 4. In order to reduce the total time required to conduct the

tests, effect of area ratio between CFS and MFI filters needs to be determined. When CFS was operated without permeate flux restriction, it took only five minutes to collect enough water for sequent SDI/MFI measurement. The SDI/MFI of the CFS permeate collected in such a short time was almost identical to that of DI water. The instant contamination or leaching from the CFS equipment was minimum compared the accumulated contamination over the seven hours of operation.

#### *4.2. Control experiment with deionized water and sodium hypochlorite*

Sodium hypochlorite solution was added to the deionized water to check the effectiveness of contamination control. As shown in Figure 5, the SDI/MFI of deionized water with 5 ppm chlorine remained similar after seven hours of CFS operation. This indicates that chlorination is necessary to eliminate the biological contamination when running CFS at current hydrodynamic conditions. As a result, the cleaning and operation procedures of CFS were determined as followed:

##### 1. CFS Cleaning

- Prepare ten liters of deionized water with free chlorine concentration of 5ppm
- Add chlorinated water to CFS feed tank and flush out system for 5 to 10 minutes
- Insert CFS microsieve into the cross-flow unit and flush system again with chlorinated deionized water for 5 to10 minutes
- Drain feed tank

##### 2. CFS Run

- Set aside 2.5 liters of feed water for “No CFS” SDI/MFI measurements
- Add remaining feedwater (approximately 10L) to CFS feed tank and add sodium hypochlorite stock solution
- Measure free chlorine concentration and adjust to 5 ppm residual
- Run system at cross-flow velocity of 1 m/s and permeate flux of 14 gfd
- Discard initial 500mL concentrate and 30mL permeate
- Run system until 2.5 liters of permeate attained
- Shut off system and drain tank/pipes of water

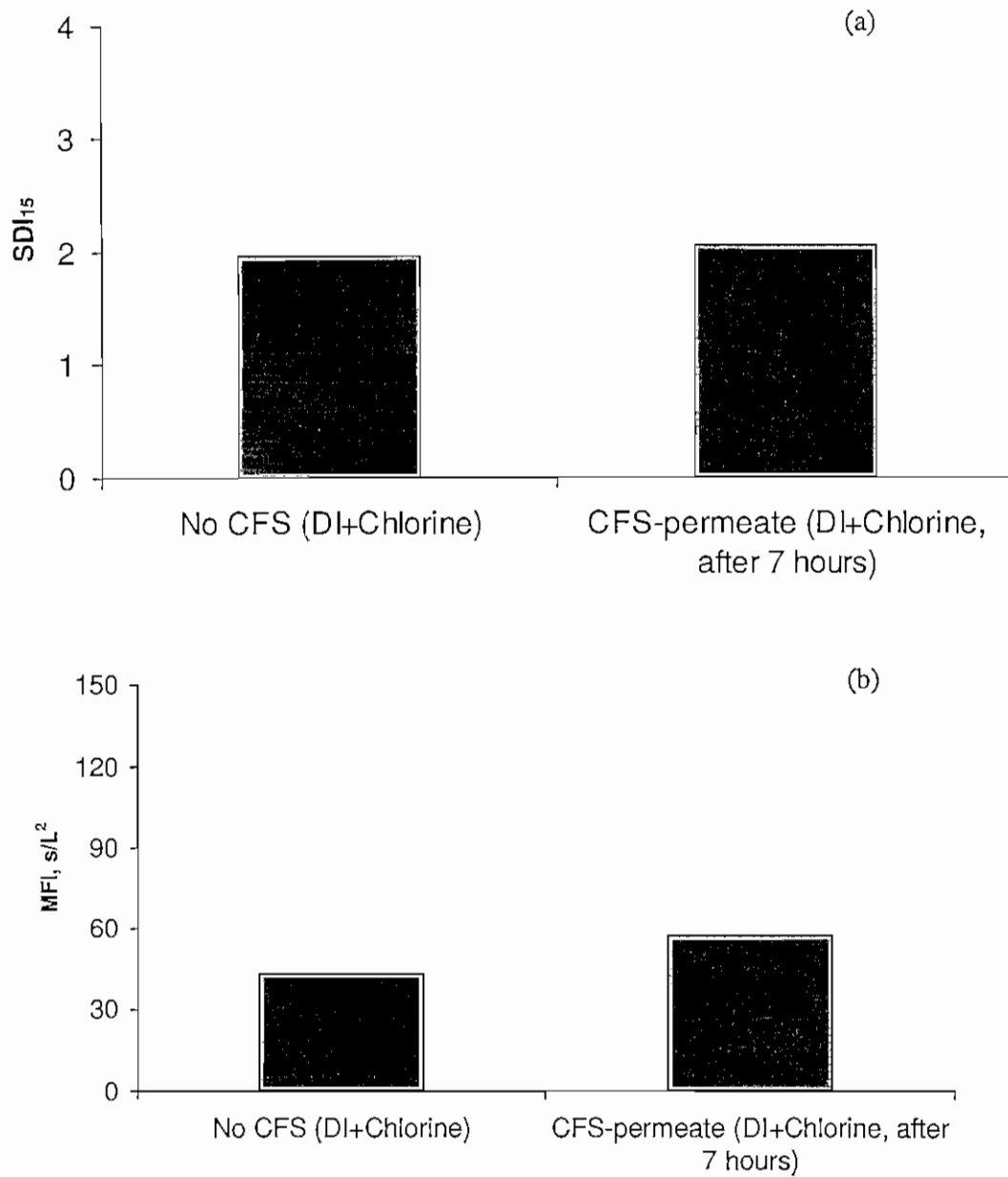


**Figure 5.** SDI (a) and MFI (b) measurements for control experiment with DI water and chlorine.

## 5. RESULTS AND DISCUSSION

### 5.1. Influence of conventional pretreatment

The SDI and MFI measurements for 1  $\mu\text{m}$  prefiltered San Diego Bay seawater and SPW surface water before and after the use of CFS are shown in Figures 6(a) and (b). Both the source waters were filtered through a 1  $\mu\text{m}$  cartridge filter before the measurements. Pretreatment using 1  $\mu\text{m}$  filters were conducted to simulate conventional pretreatment. Conventional pretreatment of surface and seawater can include coagulation/flocculation, settling, sand filtration, granular media filtration or a combination of the above technologies. For all the experiments conducted (before and after CFS), the SDI and MFI values are lower for seawater when compared to surface water. Both seawater and surface water consist of varying levels of particulate matter. The SDI measurements on raw seawater were  $\sim 5.3$  whereas the SDI of raw surface water was  $\sim 6.5$ . Thus, a higher raw SDI value for the surface water led to higher SDI and MFI values when compared to seawater.

For both the water types, a decreasing trend in SDI and MFI values are obtained after the use of CFS. Although only a marginal decrease in the SDI value was obtained after the use of CFS for surface water, the MFI values decreased significantly. Since MFI values represent cake filtration regime, they are more sensitive than SDI measurements. A significant decrease in MFI values for both source water types could have occurred due a narrower particle size distribution and a decrease in the concentration of particles after the use of CFS. Dynamic light scattering (DLS) analysis was conducted using a particle size analyzer (Brookhaven, NY) but a particle size distribution was not obtained possibly due to the lesser number of particles present after the water samples were pretreated. A more robust method to determine the particle size distribution in dilute samples will be considered as part of the future study. Since SDI and MFI values were conducted using a 0.45  $\mu\text{m}$  filter, pretreatment using a 1  $\mu\text{m}$  filter results in a particle size distribution in the range  $1 \mu\text{m} < d_p < 0.45 \mu\text{m}$ . The CFS experiments were conducted with similar hydrodynamic (cross flow and permeation) conditions present in RO processes. Hydrodynamic shear force (eq. 4) is a function of cross flow velocity and particle size. Permeation drag force is a function of permeation velocity and particle size. Since the cross flow hydrodynamic force and permeation drag force is dependant on the particle size, a greater influence of hydrodynamic forces will occur for the particle size distribution obtained after 1  $\mu\text{m}$  prefiltration. Thus, pretreatment of the source water with a 1  $\mu\text{m}$  prefilter could result in a narrower particle size distribution. A more uniform size distribution of particles will lead to a uniform porosity of the cake layer formed on the 0.45  $\mu\text{m}$  filter and hence lead to higher flux through the filter. Thus, the MFI values are significantly different for both source water types after the use of CFS.

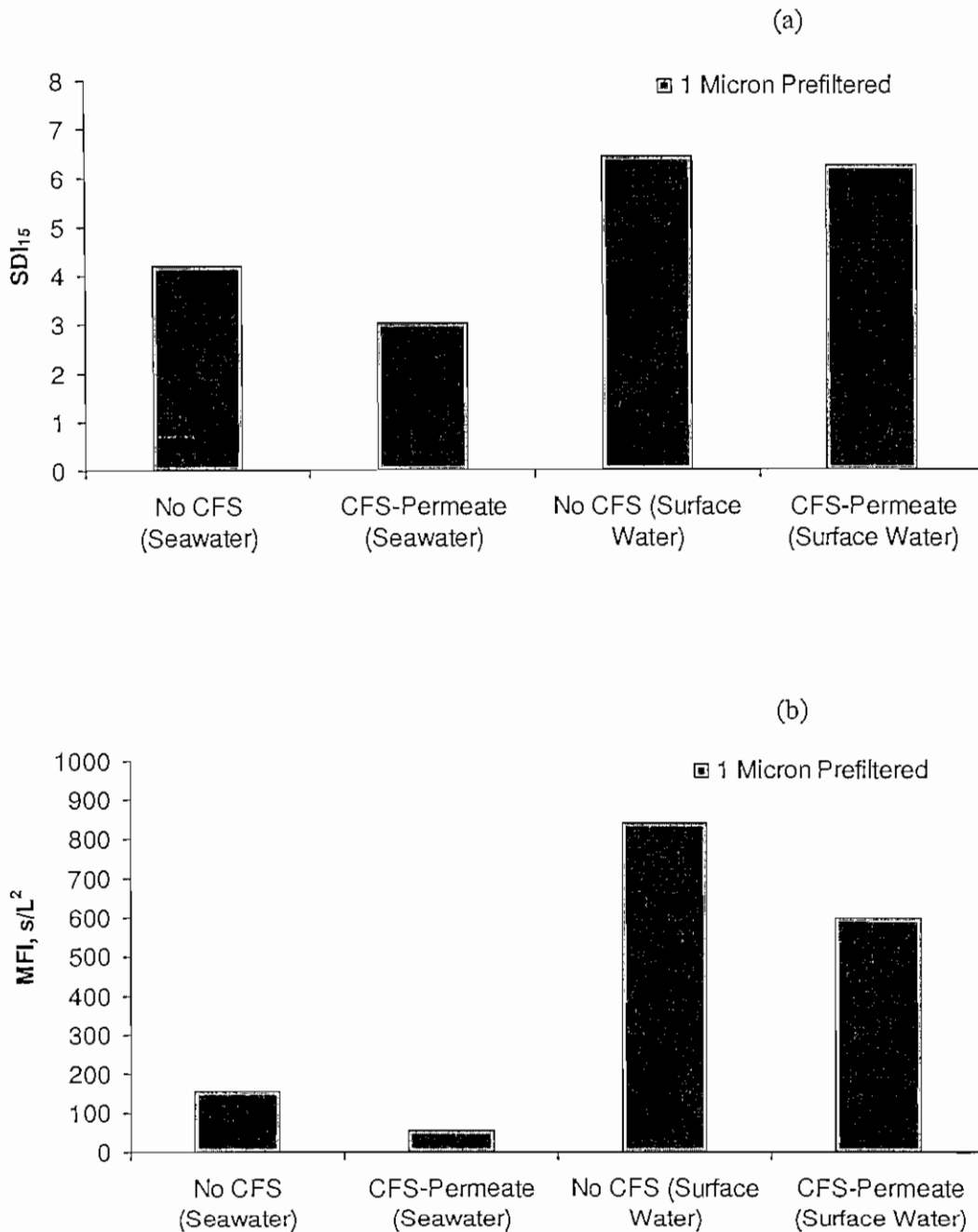


**Figure 6.** Influence of conventional (1  $\mu\text{m}$ ) pretreatment on SDI (a) and MFI (b) measurements for San Diego bay seawater and SPW surface water before and after CFS. Number of experiments conducted for each source water,  $n = 2$ .

Due to higher volume of permeate collected (lower SDI and MFI) when fouling indices tests were conducted after the CFS, it is hypothesized that a more uniform particle size distribution is obtained after the CFS. Due to the presence of cross flow and

permeation hydrodynamics in the CFS, uniform particle size distribution can lead to a more structured cake layer formation on the membrane surface causing higher flux through the membrane filter. In the absence of the CFS, even after pretreatment techniques, a distribution of particle sizes occurs leading to a more unstructured cake layer formation on the membrane surface. In Figure 7(a) and (b) an illustration of the hypothesized phenomena is shown. An illustration of the hypothesized particle size distribution before and after the use of CFS is shown in Figure 8. Due to selective screening of particulates in the raw water a more narrow distribution is expected to occur.

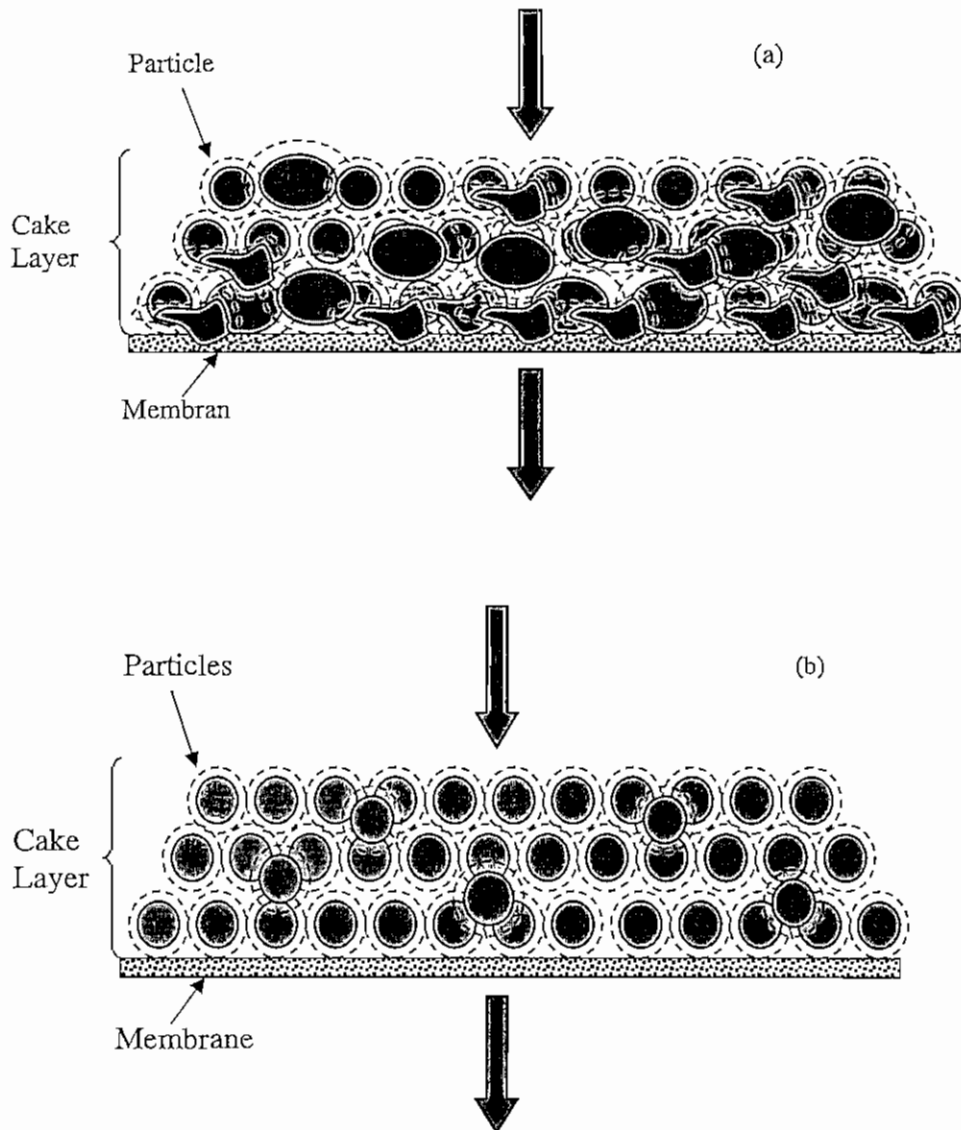


**Figure 7.** Illustration of cake layer structure in the presence of wide particle size distribution is shown in (a) and in (b) cake layer structure in the presence of uniform particle size distribution is shown.

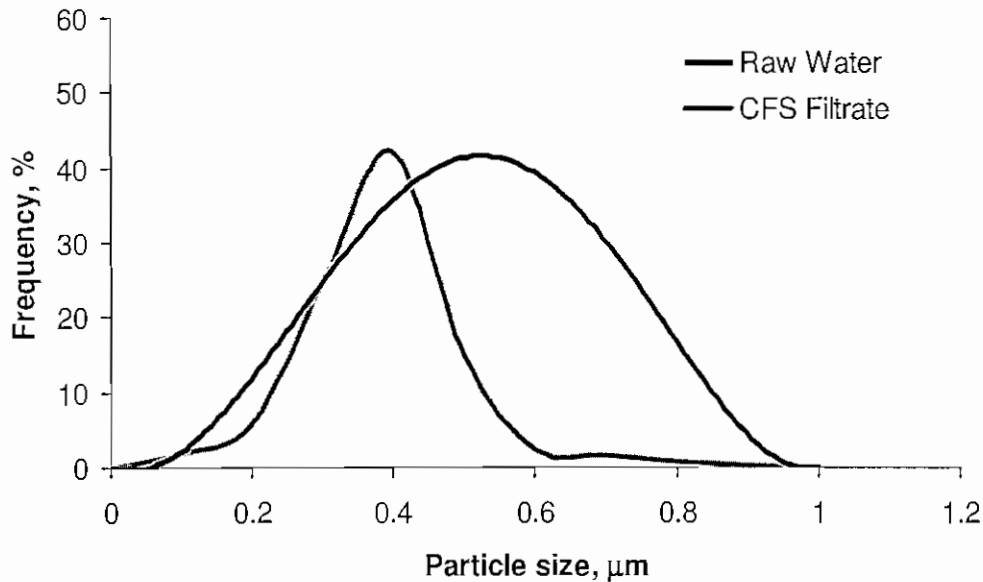


**Figure 8.** Illustration of hypothesized particle size distribution obtained from CFS filtrate.

### 5.2. Influence of loose MF/tight conventional pretreatment

The SDI and MFI measurements for 0.22 μm prefiltered San Diego Bay seawater and SPW surface water before and after the use of CFS are shown in Figures 9(a) and (b). Both the source waters were filtered through a 0.22 μm flatsheet filter before the measurements. Prefiltration through a 0.22 μm filter represents a loose MF and tight conventional pretreatment. For seawater and surface water, both SDI and MFI decrease after the use of CFS. The SDI and MFI values are higher for surface water when compared to seawater. When SDI and MFI values were conducted using a 0.45 μm filter, pretreatment using a 0.22 μm filter will result in an ideal particle size,  $d_p < 0.22 \mu\text{m}$ . Similar to previous results, a decrease in SDI and MFI occurs after the use of CFS. The SDI and MFI values is significantly lower when compared to conventional (1 μm) pretreatment due to better filtration and removal of more particulates by loose MF/tight conventional (0.22 μm) pretreatment.

### 5.3. Influence of MF pretreatment

The SDI and MFI measurements for membrane bioreactor effluent (nominal pore size ~0.1 μm) before and after the use of CFS are shown in Figures 10(a) and (b). A membrane bioreactor (MBR) was used for treating wastewater. Compared to the influence of conventional and loose MF/tight conventional pretreatment, the SDI values for the MBR effluent is not significantly different before and after the use of CFS. Since

the MFI values are more sensitive, a decrease in value is obtained after the use of CFS. After the water passes through a 0.1  $\mu\text{m}$  MBR, a nominal particle size,  $d_p < 0.1 \mu\text{m}$  is obtained. The cross flow lift and shear induced diffusion forces scale on the order of two and three times the particle diameter (eqs. 3 and 4). Thus, after pretreatment with MF membranes, the particle size in the feed is significantly smaller. Therefore, the hydrodynamic conditions in the CFS seem to have a lesser influence in segregating the particles according to size distribution. Thus, the SDI values are not significantly different after CFS when compared to SDI values without the use of CFS.

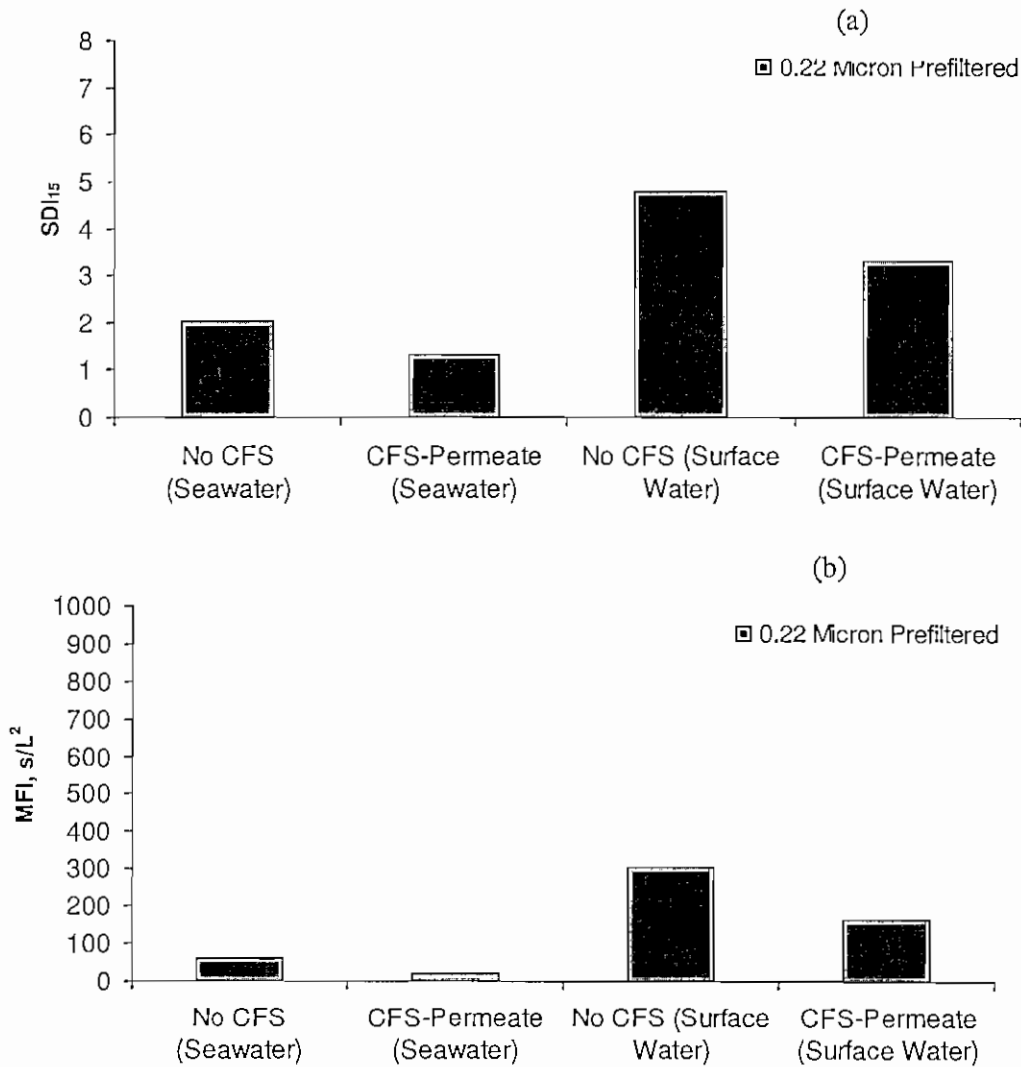


**Figure 9.** Influence of loose MF/tight conventional (0.22  $\mu\text{m}$ ) pretreatment on SDI (a) and MFI (b) measurements for San Diego bay seawater and SPW surface water before and after CFS. Number of experiments conducted for each source water,  $n = 2$ .

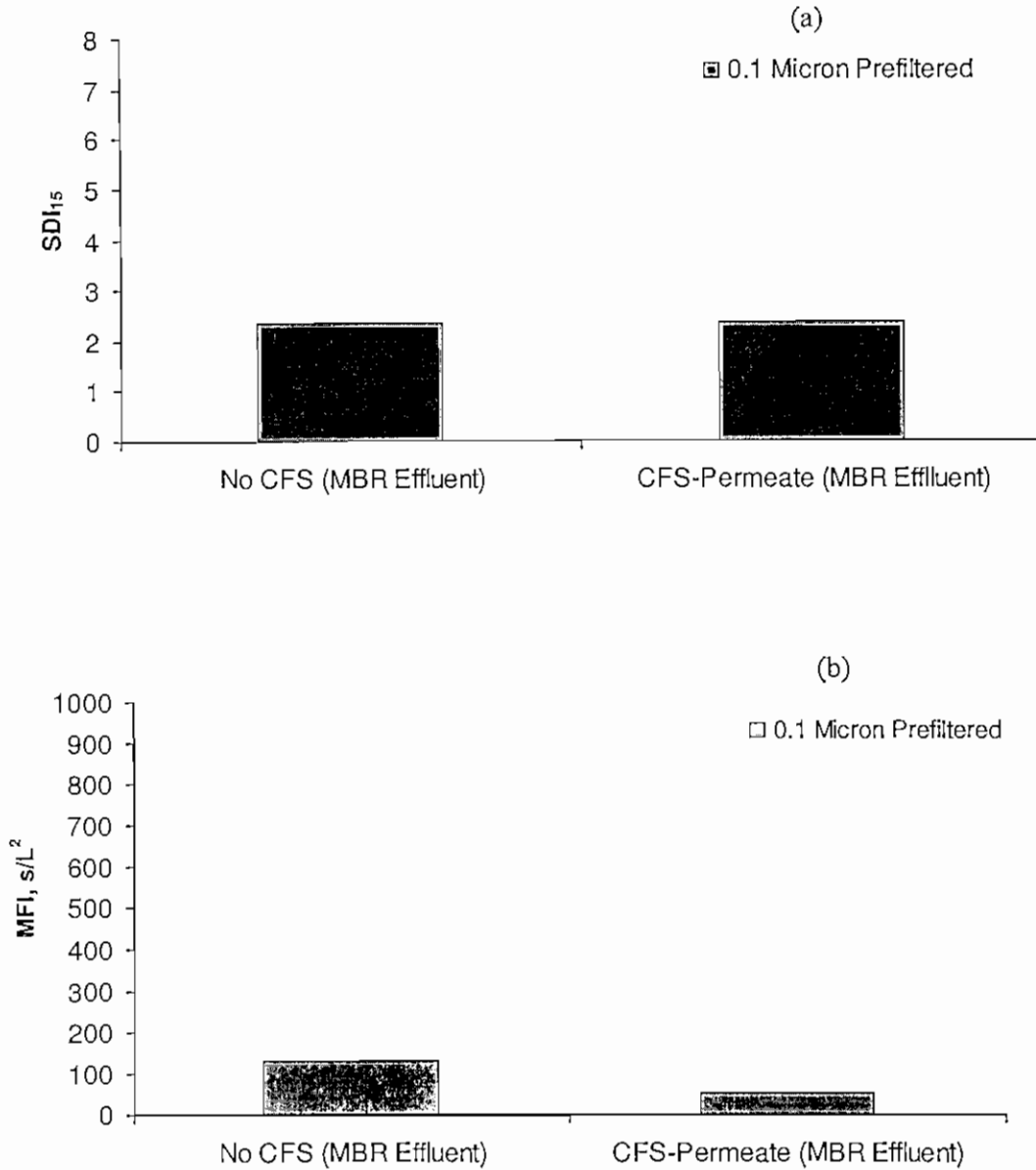


**Figure 10.** Influence of MF (0.1 μm) pretreatment on SDI (a) and MFI (b) measurements for MBR effluent before and after CFS. Number of experiments conducted for each source water,  $n = 2$ .

#### 5.4. Influence of UF pretreatment

The SDI and MFI measurements for 0.04 μm prefiltered surface water before and after the use of CFS are shown in Figures 11(a) and (b). After the water passes through a

0.04  $\mu\text{m}$  membrane filter, a nominal particle size,  $d_p < 0.04 \mu\text{m}$  is obtained. Thus, after pretreatment with tight MF/UF membranes, the particle size in the feed is significantly smaller. A further decrease in particle size does not have a significant influence on the cross flow lift and shear induced diffusion forces. In general, as the particle size decreases, Brownian diffusion forces dominate and the process is diffusion dominated. Brownian diffusion is directly proportional to water temperature and is inversely proportional to the particle size (eq. 5). Thus, as particle size in the feed water decreases Brownian diffusion plays a more dominant role when compared to hydrodynamics. Therefore, the hydrodynamic conditions in the CFS seem to have a lesser influence in segregating the particles of smaller size and the process. Thus, the SDI values are not significantly different after CFS when compared to SDI values without the use of CFS. After prefiltration with a tight MF/UF, the MFI values also do not seem to be significantly different.

The SDI values obtained before and after the use of CFS for all the source water and pretreatment types are plotted in Figure 12(a). MFI values obtained before and after the use of CFS for all the source water and pretreatment types are plotted in Figure 11(b). The straight line represents deviation of SDI/MFI values after the use of CFS. If the SDI and MFI values after the use of CFS were similar to the measured values without CFS, all the experimental data obtained from this study should collapse on the line. Thus, data points closer to the line represent values which do not deviate significantly from the conventional SDI and MFI measurements. From Figure 12(a) it is clear that the SDI values obtained after CFS with MF and tight MF/UF pretreatment are not significantly different from conventional indices measurements. Figure 12(b) compares MFI values obtained before and after the use of CFS. As the particle size decreases due to pretreatment, the MFI values obtained after CFS are very close to the values obtained without the CFS. Thus, MFI values obtained from the tight MF/UF pretreatment falls on the linear line, representing not a significant difference in indices for smaller particle size fraction. The main drawback with conventional SDI measurements is the non proportional relation to fouling behavior of RO membranes. From Figures 12(a) and (b) it is clear that the SDI and MFI values obtained with the new technique using the CFS system, is not proportional to standard SDI and MFI indices. Thus, as part of future work, the indices obtained after CFS system would be compared to flux decline behavior of various source waters to determine the sensitivity in measurements and hence predict RO flnx decline.

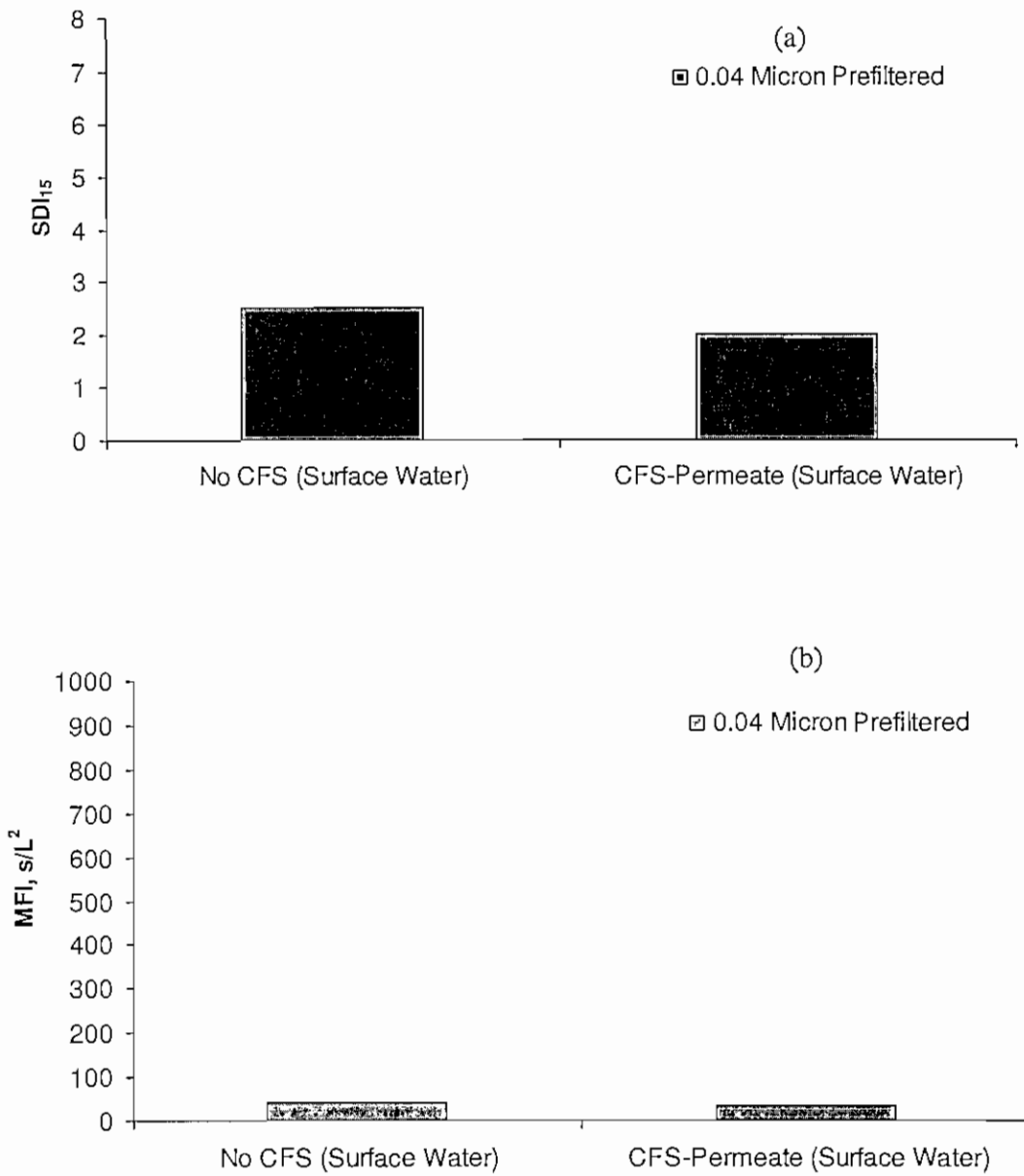


**Figure 11.** Influence of tight UF (0.04  $\mu\text{m}$ ) pretreatment on SDI (a) and MFI (b) measurements for SPW surface water before and after CFS. Number of experiments conducted for each source water,  $n = 2$ .

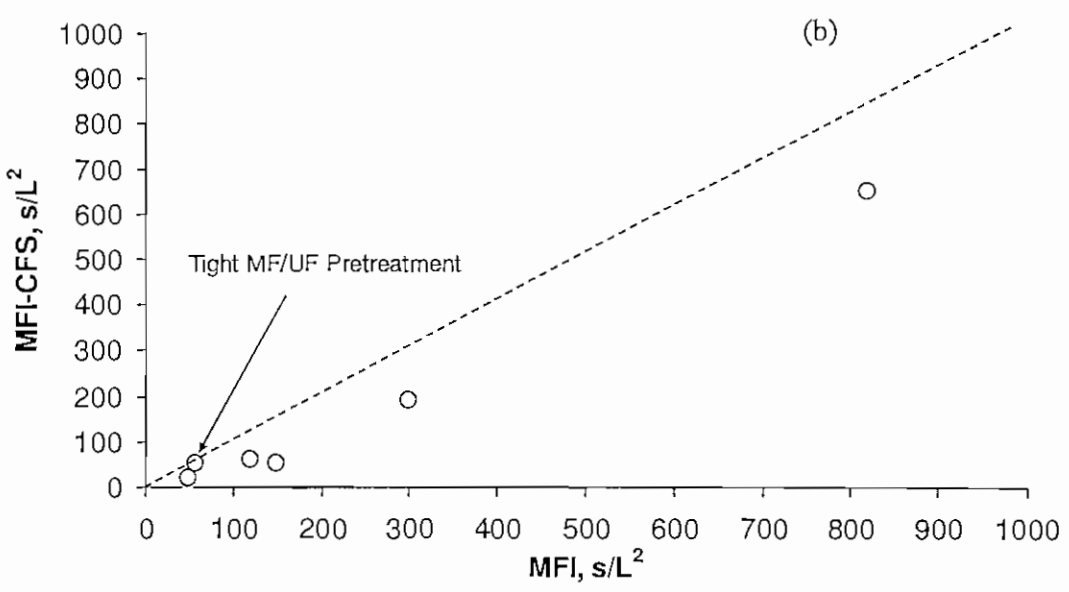
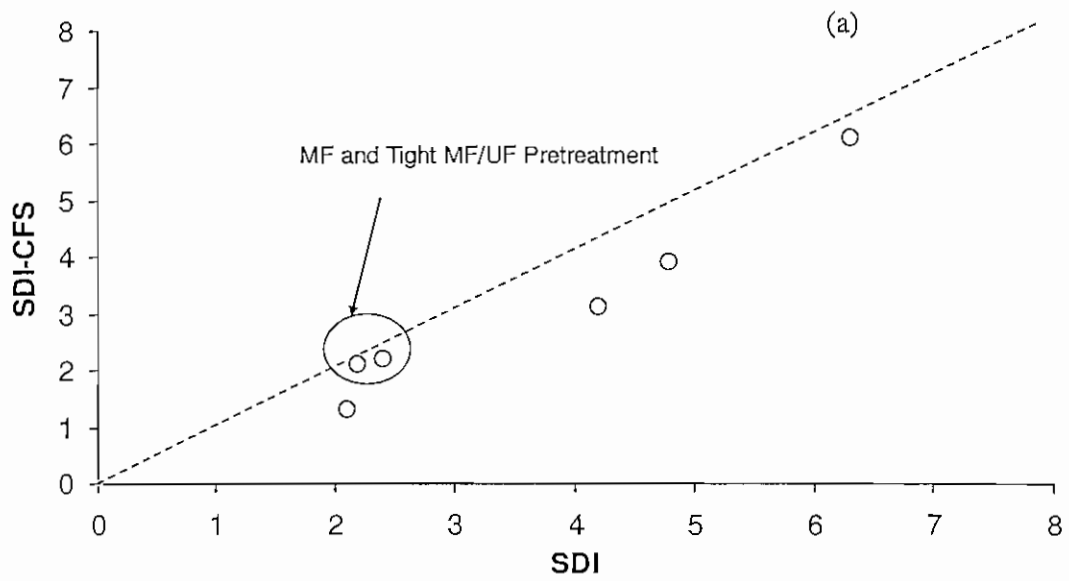


**Figure 12.** Comparison between conventional SDI and SDI-CFS measurements (a) and (b) comparison between conventional MFI and MFI-CFS measurements.

## 6. CONCLUSIONS

A new technique to systematically measure SDI and MFI was developed using a novel cross flow sampler (CFS) system. Different source water types were prefiltered through various pore size filters to obtain water representing conventional, loose MF/tight conventional, MF, and tight MF/UF pretreatments. The prefiltered water was passed through a CFS system and the permeate obtained was used to determine SDI and MFI after CFS. The CFS system was used to simulate similar hydrodynamic conditions of a RO process.

The SDI and MFI values obtained after CFS were significantly lower when for conventional and loose MF/tight conventional treated water. The SDI and MFI values were not significantly lower for tight MF/UF pretreated water. Hydrodynamic conditions incorporated in the CFS system seemed to play a critical role. Since cross flow lift and shear induced diffusion forces are a function of particle size and flowrate, larger particles from conventional and loose MF/tight conventional pretreated water encounter higher back-transport velocities. Thus, the permeate collected from the CFS system resulted in lower SDI and MFI values when compared to standard fouling indices.

When tight MF/UF pretreatment was used, a smaller size ( $d_p < 0.04 \mu\text{m}$ ) distribution in the feed is obtained leading to lower influence of hydrodynamics and dominance of Brownian diffusion. Thus, the permeate collected from the CFS system after tight MF/UF pretreatment did not result in a significant difference in SDI and MFI measurements when compared to standard fouling indices. Due to the presence of similar hydrodynamic conditions as a RO process, the SDI and MFI measurements obtained using the CFS system could serve to be a more appropriate method to measure fouling indices.

## 7. FUTURE WORK

In order further test the applicability of the newly developed method to systematically measure SDI and MFI, future work proposed is listed below.

### **Phase I:**

#### Extended Exploratory Research:

- Determine the influence of porosity of different CFS filters.
- Determine the influence of area ratio ( $A_{CFS}/A_{MFI}$ ) on MFI measurements.

### **Phase II:**

#### Prototype Development of CFS Unit:

- MFI cell directly connected to CFS permeate.
- Design continuous operation of CFS unit at constant flux and measurement of transmembrane pressure (TMP) using pressure transducers to determine MFI.

#### Foulant Characterization:

- Analysis of particle size distribution and concentration (particle count) in feed and permeate of CFS unit.
- Scanning electron microscopy (SEM) analysis of cake layer structure after SDI/MFI measurements before and after the use of CFS unit.

### **Phase III:**

#### Fouling Analysis:

- Conduct RO bench scale studies with various source waters to determine the correlation between SDI/MFI measurements after CFS and RO flux decline.
- Conduct RO bench scale studies using novel RO tester to determine cake thickness of fouling layer using ultrasonic time-domain reflectometry (UTDR) measurements and correlate with SDI/MFI measurements after CFS unit.

### **Phase IV:**

#### Full Scale Implementation of CFS unit and Testing Protocol:

- Pilot scale testing of the CFS unit with various source water types and correlating with full scale RO flux decline behavior.
- Industry participation in implementation of CFS unit in full scale plants.
- Development of a standardized test protocol to determine SDI/MFI using the CFS unit.

## REFERENCES

MWH, 2005, Water Treatment: Principles and Design, 2nd Edition, John Wiley and Sons, Inc., Hoboken, NJ.

Wiesner, M.; Clark, M., M.; Mallevalle, J., 1988, Membrane Filtration of Coagulated Suspensions, J. of Environmental Engineering, 115 (1) 22- 40.

Li., H.; Fane A.G.; Coster, H.G.L.; and Vigneswaran, S., 1998. Observation of deposition and removal behavior of submicron bacteria on the membrane surface during cross flow microfiltration, Journal of Membrane Science Vol. 217, No. 1-2, pp. 29-41.

Boerlage, Siobhàn F.E.; Kennedy, Maria D.; Aniye, Meseret Petrosa; Abogrean, Elhadi M.; El-Hodali, Dima E.Y.; Tarawneh, Zeyad S.A.; Schippers, 2000, Modified Fouling Index<sub>ultrafiltration</sub> to compare pretreatment processes of reverse osmosis feedwater, Desalination, Vol: 131, No. 1-3, pp. 201-214.

Welsch, K.; Mc Donogh, R. M.; Fane, A.G.; Fell, C. J.D., 1995, Calculation of limiting fluxes in the ultrafiltration of colloids and fine particulates, J. of Membrane Science, Vol. 99, No. 3, pp. 229-239.

ASTM International, 2002, D 4189-95, Standard Test Method for Silt Density Index (SDI) of Water.

Schippers, J.C., and Verdouw, 1980, The Modified Fouling Index, a Method of Determining the Fouling Characteristics of Water, Desalination, Vol: 32, pp. 137-148.